



Experimental and theoretical molecular and electronic structures of the *N*-oxides of pyridazine, pyrimidine and pyrazine

R. Alan Aitken^{a,*}, Bernd Fodi^b, Michael H. Palmer^{b,*}, Alexandra M.Z. Slawin^{a,*}, Jing Yang^a

^a EaStCHEM School of Chemistry, University of St Andrews, North Haugh, St Andrews, Fife, KY16 9ST, UK

^b School of Chemistry, The University of Edinburgh, West Mains Road, Edinburgh, EH9 3JJ, UK

ARTICLE INFO

Article history:

Received 7 February 2012

Received in revised form 15 April 2012

Accepted 1 May 2012

Available online 8 May 2012

ABSTRACT

The structures of pyridazine *N*-oxide, pyrimidine *N*-oxide and pyrazine *N*-oxide have been determined by X-ray diffraction for the first time. Comparison with theoretical predictions of the equilibrium structures using the B3LYP method together with a cc-pVTZ basis set, show close agreement with the structural parameters observed, and experimental dipole moments, which suggests that the charge distribution is realistic. An 'atoms in molecules' (AIM) analysis of the computed wave-functions shows total electron densities rather different from the classical picture of a dative bond, whereas the same wave-functions subjected to Mulliken analysis show a more conventional view of the electron distribution. This latter procedure allows a bond dipole analysis of the *N*-oxide charge distribution.

© 2012 Elsevier Ltd. All rights reserved.

1. Introduction

The importance of the heterocyclic amine oxides, such as pyridine *N*-oxide (**1**, Fig. 1), lies in the ring susceptibility to electrophilic substitution, where it is enhanced yielding a 4-nitro-derivative with ease.^{1,2} This contrasts with pyridine, which yields a 3-nitro-

derivative with difficulty. This is generally true of the azine *N*-oxides when a *para* position is available.¹ Less well-known is the ease of cross-coupling reactions with aryl bromides at positions *ortho* to the *N*-oxide.³ In the present paper we present structural and electron distribution results for the series of compounds **1–5** (Fig. 1). A further factor of importance for these amine oxides, is that some 4-nitro-derivatives of pyridine and quinoline *N*-oxides are active against a number of tumours.^{4,5} The dative bond shown in **6** (Fig. 1) for this series of compounds is widely used to explain¹ the reactivity of the 4-position in **1**, with similar explanations for the 2-position. This brings into focus both permanent and reaction induced properties of the ring **6**, which are discussed further below.

Although their synthesis was reported over 50 years ago,⁶ the crystalline structures of the isomeric diazine (mono) *N*-oxides **2–4** have not so far been determined. We now report the results of single-crystal X-ray diffraction studies on these three compounds. There have been no previous X-ray diffraction (XRD) studies of simple diazine *N*-oxides, but there are X-ray structures for **1**^{7,8} and **5**,⁹ as well as microwave (MW)^{10–12} and electron diffraction (ED)¹³ structures for **1**; the MW studies are by far the most detailed, since the X-ray and ED studies made a number of assumptions. These data are shown in Table 1 and are compared with the corresponding theoretical data presented here.

Structures for a few substituted pyrazine *N*-oxide,¹⁴ and pyrazine-*N,N'*-dioxides¹⁵ have been determined; a complex 1,2,5-oxadiazolo[3,4-*d*]pyridazine-5,6-dioxide¹⁶ appears to be the only example of a crystal structure with the pyridazine-*N,N'*-dioxide function present. Although originally thought unlikely owing to the adjacent positive charges, pyridazine *N,N'*-dioxides have been

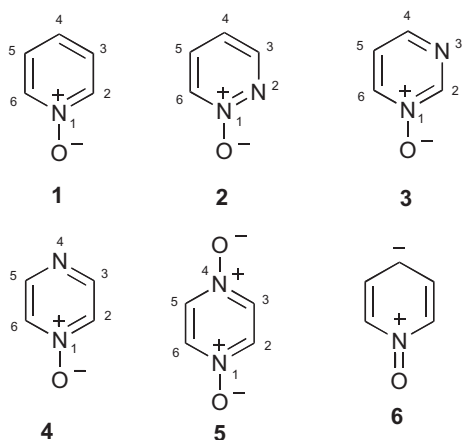


Fig. 1. Compounds studied with numbering scheme used.

* Corresponding authors. E-mail address: raa@st-and.ac.uk (R.A. Aitken).

Table 1
Comparison of experimental and theoretical bond lengths (Å) and angles (°) for pyridine *N*-oxide **1** and pyridine

| | Pyridine <i>N</i> -oxide 1 | | | | Pyridine | | |
|------------------------------------------------|-----------------------------------|--------------------|---------------------|-------|---------------------|------------------|--------|
| | XRD ^{8,a} | ED ^{13,b} | MW ^{11,44} | DFT | XRD ^{23,c} | MW ²⁴ | DFT |
| <i>Bond</i> | | | | | | | |
| N ₁ –O ₁ | 1.330 | 1.290 | 1.2806 | 1.271 | — | — | — |
| N ₁ –C ₂ | 1.348 | 1.384 | 1.3644 | 1.369 | 1.336 | 1.3376 | 1.3330 |
| C ₂ –H ₂ | 1.013 | (1.070) | 1.0775 | 1.078 | 0.979 | 1.0857 | 1.0846 |
| C ₂ –C ₃ | 1.371 | 1.381 | 1.3814 | 1.377 | 1.381 | 1.3938 | 1.3908 |
| C ₃ –H ₃ | 1.078 | (1.070) | 1.0820 | 1.081 | 0.949 | 1.0818 | 1.0815 |
| C ₃ –C ₄ | 1.375 | 1.393 | 1.3953 | 1.390 | 1.377 | 1.3916 | 1.3882 |
| C ₄ –H ₄ | 0.867 | (1.070) | 1.0787 | 1.080 | 0.964 | 1.0811 | 1.0822 |
| C ₄ –C ₅ | 1.375 | 1.393 | 1.3953 | 1.390 | 1.377 | 1.3916 | 1.3882 |
| C ₅ –H ₅ | 1.078 | (1.070) | 1.0820 | 1.081 | 0.949 | 1.0818 | 1.0815 |
| C ₅ –C ₆ | 1.371 | 1.381 | 1.3814 | 1.377 | 1.381 | 1.3938 | 1.3908 |
| C ₆ –H ₆ | 1.013 | (1.070) | 1.0775 | 1.078 | 0.979 | 1.0857 | 1.0846 |
| C ₆ –N ₁ | 1.348 | 1.384 | 1.3664 | 1.369 | 1.336 | 1.3376 | 1.3330 |
| <i>Angle</i> | | | | | | | |
| C ₂ –N ₁ –O ₁ | 119.5 | | 120.4 | 120.8 | — | — | — |
| C ₂ –N ₁ –C ₆ | 121.0 | 120.9 | 119.2 | 118.4 | 116.6 | 116.9 | 117.4 |
| N ₁ –C ₂ –C ₃ | 119.7 | 118.0 | 121.0 | 121.4 | 123.6 | 123.8 | 123.6 |
| N ₁ –C ₂ –H ₂ | 111.1 | (120.5) | 113.8 | 113.8 | 116.1 | 116.0 | 116.2 |
| H ₂ –C ₂ –C ₃ | 129.2 | (121.5) | 125.2 | 124.9 | 120.3 | 120.2 | 120.3 |
| C ₂ –C ₃ –C ₄ | 120.9 | 124.6 | 121.0 | 120.6 | 118.6 | 118.5 | 118.5 |
| C ₂ –C ₃ –H ₃ | 113.2 | (108.5) | 118.4 | 118.3 | 119.6 | 120.1 | 120.3 |
| H ₃ –C ₃ –C ₄ | 125.7 | (126.9) | 121.1 | 121.1 | 121.8 | 121.4 | 121.2 |
| C ₃ –C ₄ –C ₅ | 117.9 | 114.1 | 117.6 | 117.7 | 118.8 | 118.4 | 118.6 |
| C ₃ –C ₄ –H ₄ | 121.1 | (123.0) | 121.2 | 121.2 | 120.6 | 120.8 | 120.7 |
| H ₄ –C ₄ –C ₅ | 121.1 | (123.0) | 121.2 | 121.2 | 120.6 | 120.8 | 120.7 |
| C ₄ –C ₅ –C ₆ | 120.9 | 124.6 | 121.0 | 120.6 | 118.6 | 118.5 | 118.5 |
| C ₄ –C ₅ –H ₅ | 125.7 | (126.9) | 121.1 | 121.1 | 121.8 | 121.4 | 121.2 |
| H ₅ –C ₅ –C ₆ | 113.2 | (108.5) | 118.4 | 118.3 | 119.6 | 120.1 | 120.3 |
| C ₅ –C ₆ –N ₁ | 119.7 | 118.0 | 121.0 | 121.4 | 123.6 | 123.8 | 123.6 |
| C ₅ –C ₆ –H ₆ | 129.2 | (121.5) | 125.2 | 124.9 | 120.3 | 120.2 | 120.3 |
| H ₆ –C ₆ –N ₁ | 111.1 | (120.5) | 113.8 | 113.8 | 116.1 | 116.0 | 116.2 |

^a CCDC Ref Code PYRDNO11.

^b Values in parentheses are either assumed (lengths), or based on non-bonded distance estimates (for angles).

^c CCDC Ref Code PYRDA01—Mean of four molecules.

synthesised by direct oxidation, initially for cinnoline *N,N'*-dioxide,¹⁷ the benzo-compound, and subsequently for pyridazine *N,N'*-oxide.¹⁸

In the present study, we make comparisons between the azines and their *N*-oxides, because the structure and electron density in each pair of compounds are so different.^{19,20} Structural data have previously been determined by a range of techniques for the parent azines: pyridine,^{21–24} pyridazine,^{25–29} pyrimidine^{30–33} and pyrazine.^{30,34–36}

We also compare with the equilibrium structures determined using density functional (DFT) methods.^{37,38} The wave-functions can generate molecular properties, which are close to experiment for a number of molecules,^{37,38} hence the wave-functions produced can be compared with experimental properties such as dipole moments and ¹⁴N quadrupole coupling, giving additional checks on reliability of the calculations. All of these aspects contribute to knowledge of the nature of these polar molecules.

2. Theoretical methods

The equilibrium structures for the azines and their *N*-oxides were determined using the Gaussian-03 suite of programmes.³⁹ We use a cc-pVTZ basis set⁴⁰ with the B3LYP hybrid version of the DFT suite. The total electron densities at the atomic centres were determined by the AIM method using the AIMPAC package.^{41,42} The same wave-functions were also subjected to a classical Mulliken Analysis,⁴³ giving the results discussed later. The theoretical structures for all the compounds are presented in Fig. 2, where

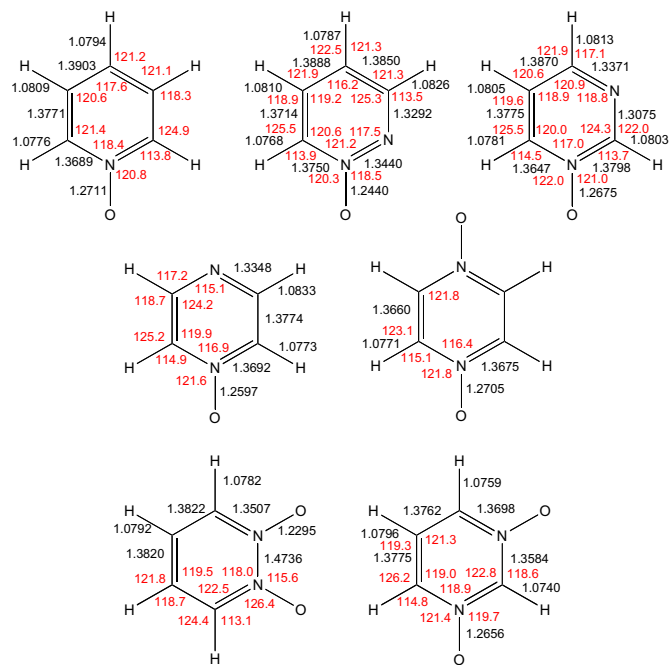


Fig. 2. Theoretical structures for the present series.

pyridazine *N,N'*-dioxide and pyrimidine *N,N'*-dioxide are shown for completeness.

Before going on to describe the new experimental structural results for compounds **2–4**, a comparison of available experimental (XRD, ED, MW) data with the results of the present theoretical equilibrium structures for the *N*-oxides **1**^{7,8} and **5**⁹ are shown in Tables 1 and 2, where the theoretical results are rounded to a similar number of significant figures to the corresponding experimental data.

3. Experimental study

Samples of the diazine *N*-oxides **2–4** were prepared by oxidation of the corresponding diazines with either *m*-chloroperbenzoic acid³ (mCPBA) or hydrogen peroxide in acetic acid.^{6,45} Compounds **3** and **4** readily formed good quality prisms suitable for X-ray diffraction upon simple recrystallisation; however, the low melting point of **2** meant that suitable crystals were only formed with great difficulty and the *R*-factor of the resulting structure is rather poorer.

The X-ray structure of pyridazine *N*-oxide **2** showed eight molecules per unit cell with two distinct molecular geometries A and B (Table 3, Fig. 3). As displayed in Fig. 3 these are centrosymmetrically arranged: $\begin{matrix} A & B & A & B \\ B & A & B & A \end{matrix}$ and there are no significant intermolecular interactions.

The X-ray structure of pyrimidine *N*-oxide **3** showed only a single molecular geometry and four molecules per unit cell (Table 4, Fig. 4).

The X-ray structure of pyrazine *N*-oxide **4** again showed eight molecules per unit cell with two distinct molecular geometries A and B (Table 5, Fig. 5).

As displayed in Fig. 5 these are arranged:

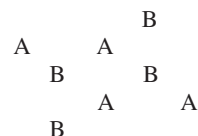


Table 2
Comparison of theoretical and experimental bond lengths (Å) and angles (°) for pyrazine-di-*N*-oxide **5** and pyrazine

| | Pyrazine-di- <i>N</i> -oxide 5 | | Pyrazine | | |
|------------------------------------------------|---------------------------------------|--------|---------------------|------------------|--------|
| | XRD ^{9,a} | DFT | XRD ^{35,b} | ED ³⁰ | DFT |
| <i>Bond</i> | | | | | |
| N ₁ –O ₁ | 1.296 | 1.2705 | — | — | — |
| N ₁ –C ₂ | 1.353 | 1.3675 | 1.333 | 1.339 | 1.3320 |
| C ₂ –H ₂ | 0.930 | 1.0771 | 0.939 | 1.115 | 1.0839 |
| C ₂ –C ₃ | 1.362 | 1.3660 | 1.388 | 1.403 | 1.3906 |
| C ₃ –H ₃ | 0.930 | 1.0771 | 0.939 | 1.115 | 1.0839 |
| C ₃ –N ₄ | 1.358 | 1.3675 | 1.333 | 1.339 | 1.3320 |
| N ₄ –O ₄ | 1.296 | 1.2705 | — | — | — |
| N ₄ –C ₅ | 1.353 | 1.3675 | 1.333 | 1.339 | 1.3320 |
| C ₅ –H ₅ | 0.930 | 1.0771 | 0.939 | 1.115 | 1.0839 |
| C ₅ –C ₆ | 1.362 | 1.3660 | 1.388 | 1.403 | 1.3906 |
| C ₆ –H ₆ | 0.930 | 1.0771 | 0.939 | 1.115 | 1.0839 |
| C ₆ –N ₁ | 1.358 | 1.3675 | 1.333 | 1.339 | 1.3320 |
| <i>Angle</i> | | | | | |
| C ₂ –N ₁ –O ₁ | 121.1 | 121.8 | — | — | — |
| C ₆ –N ₁ –O ₁ | 120.6 | 121.8 | — | — | — |
| C ₂ –N ₁ –C ₆ | 118.3 | 116.4 | 116.2 | 115.6 | 116.1 |
| N ₁ –C ₂ –C ₃ | 120.9 | 121.8 | 121.9 | 122.2 | 122.0 |
| N ₁ –C ₂ –H ₂ | 119.6 | 115.1 | 115.9 | 113.9 | 117.2 |
| H ₂ –C ₂ –C ₃ | 119.5 | 123.1 | 122.1 | 123.9 | 120.9 |
| C ₂ –C ₃ –N ₄ | 120.8 | 121.8 | 121.9 | 122.2 | 122.0 |
| C ₂ –C ₃ –H ₃ | 119.6 | 123.1 | 122.1 | 123.9 | 120.9 |
| H ₃ –C ₃ –N ₄ | 119.6 | 115.1 | 115.9 | 113.9 | 117.2 |
| C ₃ –N ₄ –C ₅ | 118.3 | 116.4 | 116.2 | 115.6 | 116.1 |
| C ₃ –N ₄ –O ₄ | 120.6 | 121.8 | — | — | — |
| O ₄ –N ₄ –C ₅ | 121.1 | 121.8 | — | — | — |
| N ₄ –C ₅ –C ₆ | 120.9 | 121.8 | 121.9 | 122.2 | 122.0 |
| N ₄ –C ₅ –H ₅ | 119.6 | 115.1 | 115.9 | 113.9 | 117.2 |
| H ₅ –C ₅ –C ₆ | 119.5 | 123.1 | 122.1 | 123.9 | 120.9 |
| C ₅ –C ₆ –N ₁ | 120.8 | 121.8 | 121.9 | 122.2 | 122.0 |
| C ₅ –C ₆ –H ₆ | 119.6 | 123.1 | 122.1 | 123.9 | 120.9 |
| H ₆ –C ₆ –N ₁ | 119.6 | 115.1 | 115.9 | 113.9 | 117.2 |

^a CCDC Ref Code AHMAB.

^b CCDC Ref Code PYRAZI01.

Table 3
Comparison of theoretical and experimental bond lengths (Å) and angles (°) for pyridazine *N*-oxide **2** and pyridazine

| | Pyridazine <i>N</i> -oxide 2 | | | Pyridazine | | |
|------------------------------------------------|-------------------------------------|-------|-------|---------------------|------------------------|--------|
| | XRD A | XRD B | DFT | XRD ^{25,a} | MW/ED ^{28,29} | DFT |
| <i>Bond</i> | | | | | | |
| N ₁ –O ₁ | 1.242 | 1.278 | 1.244 | — | — | — |
| N ₁ –N ₂ | 1.357 | 1.359 | 1.344 | 1.346 | 1.3370 | 1.3295 |
| N ₂ –C ₃ | 1.330 | 1.304 | 1.329 | 1.325 | 1.3379 | 1.3296 |
| C ₃ –H ₃ | 0.951 | 0.950 | 1.083 | 0.979 | 1.0787 | 1.0831 |
| C ₃ –C ₄ | 1.384 | 1.373 | 1.385 | 1.395 | 1.4000 | 1.3926 |
| C ₄ –H ₄ | 0.950 | 0.951 | 1.079 | 0.934 | 1.0707 | 1.0813 |
| C ₄ –C ₅ | 1.351 | 1.373 | 1.389 | 1.371 | 1.3846 | 1.3779 |
| C ₅ –H ₅ | 0.951 | 0.951 | 1.081 | 0.945 | 1.0707 | 1.0813 |
| C ₅ –C ₆ | 1.378 | 1.367 | 1.372 | 1.390 | 1.4000 | 1.3779 |
| C ₆ –H ₆ | 0.950 | 0.950 | 1.077 | 0.988 | 1.0787 | 1.0831 |
| C ₆ –N ₁ | 1.377 | 1.350 | 1.375 | 1.330 | 1.3379 | 1.3296 |
| <i>Angle</i> | | | | | | |
| N ₂ –N ₁ –O ₁ | 118.5 | 116.7 | 118.5 | — | — | — |
| C ₆ –N ₁ –O ₁ | 120.7 | 121.6 | 120.3 | — | — | — |
| C ₆ –N ₁ –N ₂ | 120.8 | 121.6 | 121.2 | 119.3 | 119.4 | 119.5 |
| N ₁ –N ₂ –C ₃ | 117.7 | 116.5 | 117.5 | 118.9 | 119.4 | 119.5 |
| N ₂ –C ₃ –C ₄ | 124.4 | 126.2 | 125.3 | 123.9 | 123.7 | 123.7 |
| N ₂ –C ₃ –H ₃ | 118.0 | 116.8 | 113.4 | 115.5 | 114.9 | 115.1 |
| H ₃ –C ₃ –C ₄ | 117.7 | 117.0 | 121.3 | 120.6 | 121.3 | 121.3 |
| C ₃ –C ₄ –C ₅ | 117.1 | 116.0 | 116.2 | 117.1 | 116.9 | 116.9 |
| C ₃ –C ₄ –H ₄ | 121.5 | 122.0 | 121.3 | 120.1 | 120.7 | 120.9 |
| H ₄ –C ₄ –C ₅ | 121.4 | 122.0 | 122.5 | 122.8 | 122.4 | 122.2 |
| C ₄ –C ₅ –C ₆ | 120.5 | 119.5 | 119.2 | 116.9 | 116.9 | 116.9 |
| C ₄ –C ₅ –H ₅ | 119.7 | 120.2 | 121.9 | 123.8 | 122.4 | 122.2 |
| H ₅ –C ₅ –C ₆ | 119.8 | 120.3 | 118.9 | 119.3 | 120.7 | 120.9 |
| C ₅ –C ₆ –N ₁ | 119.6 | 120.2 | 120.6 | 123.9 | 123.8 | 123.7 |
| C ₅ –C ₆ –H ₆ | 120.2 | 119.9 | 125.5 | 120.0 | 121.3 | 121.3 |
| H ₆ –C ₆ –N ₁ | 120.2 | 119.9 | 113.9 | 116.1 | 114.9 | 115.1 |

^a CCDC Ref Code VOBJEB.

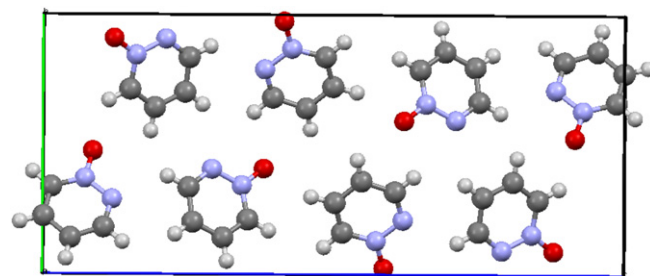


Fig. 3. Unit cell of pyridazine *N*-oxide **2** (viewed along *a*-axis).

Table 4
Comparison of theoretical and experimental bond lengths (Å) and angles (°) for pyrimidine *N*-oxide **3** and pyrimidine

| | Pyrimidine <i>N</i> -oxide 3 | | Pyrimidine | | |
|------------------------------------------------|-------------------------------------|--------|---------------------|------------------------------------|--------|
| | XRD | DFT | XRD ^{31,a} | MW ³² /ED ³⁰ | DFT |
| <i>Bond</i> | | | | | |
| N ₁ –O ₁ | 1.308 | 1.2674 | — | — | — |
| N ₁ –C ₂ | 1.359 | 1.3796 | 1.331 | 1.317 | 1.3322 |
| C ₂ –H ₂ | 0.950 | 1.0802 | 1.010 | 1.097 | 1.0842 |
| C ₂ –N ₃ | 1.315 | 1.3071 | 1.337 | 1.329 | 1.3322 |
| N ₃ –C ₄ | 1.347 | 1.3370 | 1.339 | 1.351 | 1.3322 |
| C ₄ –H ₄ | 0.951 | 1.0813 | 0.959 | 1.096 | 1.0807 |
| C ₄ –C ₅ | 1.375 | 1.3870 | 1.387 | 1.394 | 1.3871 |
| C ₅ –H ₅ | 0.950 | 1.0805 | 0.921 | 1.098 | 1.0844 |
| C ₅ –C ₆ | 1.369 | 1.3774 | 1.388 | 1.393 | 1.3871 |
| C ₆ –H ₆ | 0.950 | 1.0781 | 0.966 | 1.087 | 1.0844 |
| C ₆ –N ₁ | 1.359 | 1.3649 | 1.337 | 1.361 | 1.3322 |
| <i>Angle</i> | | | | | |
| C ₂ –N ₁ –O ₁ | 119.9 | 121.0 | — | — | — |
| C ₆ –N ₁ –O ₁ | 121.4 | 122.0 | — | — | — |
| C ₂ –N ₁ –C ₆ | 118.7 | 117.0 | 115.9 | 116.0 | 116.0 |
| N ₁ –C ₂ –N ₃ | 124.0 | 124.3 | 126.8 | 127.8 | 127.0 |
| N ₁ –C ₂ –H ₂ | 118.0 | 113.7 | 115.3 | 116.1 | 116.5 |
| H ₂ –C ₂ –N ₃ | 118.0 | 122.0 | 117.9 | 116.1 | 116.5 |
| C ₂ –N ₃ –C ₄ | 117.3 | 118.8 | 116.3 | 116.0 | 116.0 |
| N ₃ –C ₄ –C ₅ | 122.0 | 121.0 | 121.9 | 121.2 | 122.2 |
| N ₃ –C ₄ –H ₄ | 119.0 | 117.1 | 113.9 | 117.9 | 116.6 |
| H ₄ –C ₄ –C ₅ | 119.1 | 121.9 | 124.0 | 120.9 | 121.2 |
| C ₄ –C ₅ –C ₆ | 118.9 | 118.9 | 116.5 | 117.9 | 116.6 |
| C ₄ –C ₅ –H ₅ | 120.6 | 121.5 | 118.9 | 125.0 | 121.7 |
| H ₅ –C ₅ –C ₆ | 120.6 | 119.6 | 124.6 | 125.0 | 121.7 |
| C ₅ –C ₆ –N ₁ | 119.1 | 120.0 | 122.6 | 121.2 | 122.2 |
| C ₅ –C ₆ –H ₆ | 120.5 | 125.5 | 124.7 | 120.9 | 121.2 |
| H ₆ –C ₆ –N ₁ | 120.4 | 114.5 | 112.5 | 117.9 | 117.9 |

^a CCDC Ref Code PRMDIN01.

4. Discussion of the theoretical study

4.1. Correlation of theory and experimental structures

The calculated azine *N*-oxide data is shown in Fig. 2. In order to gain some insight into the general reliability of the theoretical method for this type of compound, and hence its predictive value, we show a comparison with other spectral data in the Tables 1–5.

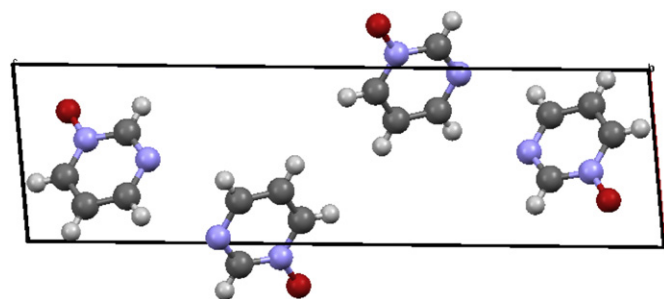


Fig. 4. Unit cell of pyrimidine *N*-oxide **3** (viewed along *b* axis).

Table 5
Comparison of theoretical and experimental bond lengths (Å) and angles (°) for pyrazine *N*-oxide **4** and pyrazine

| | Pyrazine <i>N</i> -oxide 4 | | | Pyrazine | |
|------------------------------------------------|-----------------------------------|-------|--------|---------------------|-------|
| | XRD A | XRD B | DFT | XRD ^{35,a} | DFT |
| <i>Bond</i> | | | | | |
| N ₁ –O ₁ | 1.293 | 1.272 | 1.2597 | — | — |
| N ₁ –C ₂ | 1.364 | 1.359 | 1.3692 | 1.333 | 1.332 |
| C ₂ –H ₂ | 0.951 | 0.950 | 1.0773 | 0.939 | 1.084 |
| C ₂ –C ₃ | 1.362 | 1.359 | 1.3774 | 1.388 | 1.391 |
| C ₃ –H ₃ | 0.949 | 0.949 | 1.0833 | 0.939 | 1.084 |
| C ₃ –N ₄ | 1.340 | 1.348 | 1.3348 | 1.333 | 1.332 |
| N ₄ –C ₅ | 1.339 | 1.348 | 1.3348 | 1.333 | 1.332 |
| C ₅ –H ₅ | 0.951 | 0.950 | 1.0833 | 0.939 | 1.084 |
| C ₅ –C ₆ | 1.372 | 1.359 | 1.3774 | 1.388 | 1.391 |
| C ₆ –H ₆ | 0.950 | 0.950 | 1.0773 | 0.939 | 1.084 |
| C ₆ –N ₁ | 1.355 | 1.363 | 1.3692 | 1.333 | 1.332 |
| <i>Angle</i> | | | | | |
| C ₂ –N ₁ –O ₁ | 120.4 | 121.0 | 121.6 | — | — |
| C ₆ –N ₁ –O ₁ | 121.3 | 121.3 | 121.6 | — | — |
| C ₆ –N ₁ –C ₂ | 118.3 | 117.8 | 116.9 | 116.2 | 116.1 |
| N ₁ –C ₂ –C ₃ | 119.0 | 119.3 | 119.8 | 121.9 | 122.0 |
| N ₁ –C ₂ –H ₂ | 120.5 | 120.4 | 114.9 | 115.9 | 117.2 |
| H ₂ –C ₂ –C ₃ | 120.6 | 120.3 | 125.2 | 122.1 | 120.9 |
| C ₂ –C ₃ –N ₄ | 124.9 | 125.0 | 124.2 | 121.9 | 122.0 |
| C ₂ –C ₃ –H ₃ | 117.6 | 117.5 | 118.7 | 122.1 | 120.9 |
| H ₃ –C ₃ –N ₄ | 117.5 | 117.6 | 117.2 | 115.9 | 117.2 |
| C ₃ –N ₄ –C ₅ | 114.3 | 113.8 | 115.0 | 116.2 | 116.1 |
| N ₄ –C ₅ –C ₆ | 124.2 | 124.3 | 124.2 | 121.9 | 122.0 |
| N ₄ –C ₅ –H ₅ | 117.9 | 117.9 | 117.2 | 115.9 | 117.2 |
| H ₅ –C ₅ –C ₆ | 117.9 | 117.8 | 118.7 | 122.1 | 120.9 |
| C ₅ –C ₆ –N ₁ | 119.3 | 119.8 | 119.8 | 121.9 | 122.0 |
| C ₅ –C ₆ –H ₆ | 120.3 | 120.1 | 125.2 | 122.1 | 120.9 |
| H ₆ –C ₆ –N ₁ | 120.4 | 120.1 | 114.9 | 115.9 | 117.2 |

^a CCDC Ref Code PYRAZ01.

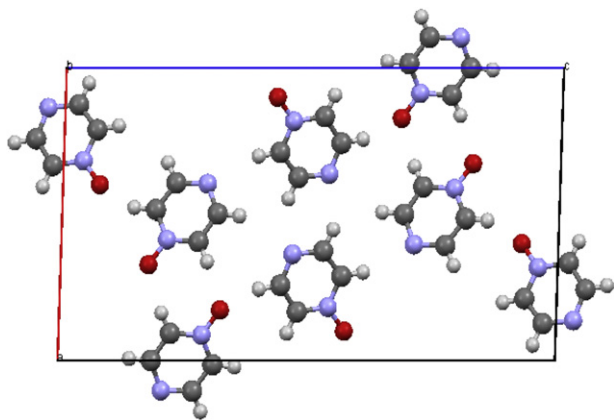


Fig. 5. Unit cell of pyrazine *N*-oxide **4** (viewed along *b* axis).

In this Section, we will correlate theory and experiment using the equation $y_{\text{Calcd}}=A+Bx_{\text{Obsd}}$, giving the correlation coefficient (*R*) and overall standard deviation (*SD*). In these data, *SD* for the parameters (*A*/*B*) is shown in parentheses.

Easily the best fit for the theoretical and experimental results is with the microwave (MW) structural data (Tables 1–5). For 43 MW bond lengths (Å), we have the linear correlation Equation above with *A* 0.020(11), *B* 0.981(8), *R* 0.9985, *SD* 7.8×10^{-3} . The bond angles for the azines have a range from 115° to 128°. Using the same Equation, a similar fit between theoretical bond angles and experimental MW values, yields, *A* 1.938 (2644), *B* 0.984 (22), *R* 0.9876, *SD* 0.449 over 52 points. Since the *SD* for the intercept in this angle correlation is larger than its intercept, the line passes through the origin, while that for the bond lengths lies close to the origin. However, if we include the larger group of azine data (41 bond measurements) where most is by electron diffraction (ED),

then the fits are somewhat poorer, with *A* 0.079(60), *B* 1.135(48), *R* 0.967 and *SD* 0.042 for the bond lengths.

Clearly, the theoretical study relates to isolated molecules, and the MW and ED studies are more relevant than X-ray studies of the solid state. If we correlate the X-ray bond length data with the theoretical results (Tables 1–5) for the azines, then the coefficients are *A* –0.041(51), *B* 1.028(38) with *R* 0.982, *SD* 0.006 over 30 points; this is still clearly acceptable. However, a correlation over all X-ray data for the four *N*-oxides gives *A* –0.412(128), *B* 1.309(95), *R* 0.940, *SD* 0.014 over 27 discrete points. This is little changed (*R* 0.959, *SD* 0.013) by removal of the older X-ray data⁷ for **1**. The fit of the azine *N*-oxides angles is: *A* 19.4(78), *B* 0.84(7), *R* 0.899, *SD* 0.97 over 41 angles. Almost all differences between theory and experiment are less than 2°, and this must be seen as a satisfactory result. The wider correlation over all 58 angles in azines and *N*-oxides is: $y_{\text{Calcd}}=A+Bx_{\text{Obsd}}$, with *A* –7.8(50), and *B* 1.07(4), with correlation coefficient *R* 0.959 and overall *SD* 0.856. Easily the worst discrepancy is with the C(4)–C(5)–H(5) angle in pyrimidine, where the present data suggests the presence of an error in the ED publication.

Hence, as expected, we conclude (a) that the difference between the calculated and X-ray structural results arise from solid state effects. (b) Clearly the MW correlations are excellent, and we anticipate that future MW studies of the *N*-oxides will give very similar values to the present calculated data.

4.2. Structural variations

Both theory (Fig. 2) and experiment (Tables 1–5) show that the bond lengths (Å) have comparatively narrow ranges in the mono *N*-oxides, with N–O 1.25 to 1.27, C–N 1.33 to 1.38 and C–C 1.37 to 1.39 Å. The longest C–C bonds lie furthest from the *N*-oxide group, as in the 3,4-bond (**2**) and 4,5-bond (**3**), respectively. The theoretical C–H bond lengths, show systematic variation, with the longest bonds (>1.08 Å) being *meta* to the *N*-oxide group. Overall the median difference between theory (T) and experiment (E) ('the error') for the bond lengths is (E–T): –0.011 (C–C), +0.006 (C–N) and +0.029 Å (N–O). Clearly all the calculated N–O bond lengths are slightly too long by this theoretical method.

The theoretical N–O bond length is more variable in the di-*N*-oxides, being shortest in the case of pyridazine di-*N*-oxide. The N–N bond lengths of the mono- and di-*N*-oxides of pyridazine show a major difference, with lengths of 1.344 and 1.473 Å, respectively. Clearly the latter shows a lengthening towards ring opening,⁴⁶ which would ultimately lead to the di-nitroso-compound. However, this structure (Fig. 2) is rather different from that for the *cis*- or *trans*-dimers of nitrosomethane,⁴⁷ where the NN, CN and NO bonds are 1.31, 1.31 and 1.47 Å, respectively. In the *N*-oxides studied, by theory and/or experiment, the ring angle at the *N*-oxide group is significantly less than 120°, with pyridazine *N*-oxide as the sole exception. Similarly, the ring angle *para* to the *N*-oxide is also smaller than 120°, with the result that the other internal ring angles are larger than 120°. In all cases of the theoretical structures, the *cis*-group O–N–C–H has an NCH angle lower than 120° by 10–12° when compared with the angle on the opposite side of the HC bond. This is not found with all the present X-ray structures, but this may be a result of the poorly defined position of the H-atoms.

4.3. Electron density considerations

The overall electron distributions as measured by the molecular dipole moments (Table 6) are very close between experimental (*X*) and present theoretical (*Y*) values. A linear correlation has $Y_{\text{Calcd}}=-0.077(49)+0.987(15)X_{\text{Obsd}}$, with overall correlation coefficient (*R*) 0.9993 and standard deviation (*SD*) 0.065 over the 8

Table 6
Comparison of experimental and theoretical dipole moments (Debye)

| Azine/Azine <i>N</i> -oxide | Experiment | Ref. | Theory |
|-------------------------------------|------------|-------|--------|
| Pyridine | 2.35 | 21 | 2.177 |
| Pyridazine | 4.22 | 26 | 4.105 |
| Pyrimidine | 2.334 | 32 | 2.280 |
| Pyrazine | 0.0 | — | 0.0 |
| Pyridine <i>N</i> -oxide 1 | 4.13 | 11,44 | 4.014 |
| Pyridazine <i>N</i> -oxide 2 | 5.21 | 49 | 5.087 |
| Pyrimidine <i>N</i> -oxide 3 | 3.65 | 50 | 3.514 |
| Pyrazine <i>N</i> -oxide 4 | 1.66 | 49 | 1.454 |
| Pyridazine <i>N,N'</i> -dioxide | — | — | 5.745 |
| Pyrimidine <i>N,N'</i> -dioxide | — | — | 4.039 |

points, and *SD* for the parameters in parentheses. This leads to confidence that the theoretical study is close to reality. For completeness, the values for the di-*N*-oxides are included.

The molecular dipole moments show that the substitution of C₄H in **1** by N₄ in **4** leads to a reduction in dipole moment but the effect is relatively small. This similarity extends to pyrazine di-*N*-oxide **5**. Similarly, the electron distribution in pyridazine di-*N*-oxide is relatively similar to that of its mono-*N*-oxide **2**; an exception is N₂ of the latter, where the positive charge arises from small contributions from all ring atoms. The dipole moment (in-plane) directions for the pyridazine- and pyrimidine *N*-oxides lie nearly perpendicular to the N₁–N₂ and N₁–C₂ bonds, respectively.

The present theoretical value for the DM of pyridine *N*-oxide compares favourably with a recent 6-311G(2d,2p) basis set using the BPW91 methodology (3.80 D).⁴⁸

A direct measure of electron densities is the 'Atoms in Molecules' (AIM) procedure.^{41,51} In that procedure, the total electronic wave-function, determined as densities at a grid of points, is integrated out to a defined distance (9 Å in the present cases) yielding the total electron density at the atomic centres.

The AIM electron densities for the azines and their *N*-oxides are shown as net atomic charges in Fig. 6; these were obtained by direct integration of the electron density at each nuclear site in turn, and hence are directly related to experimental electron densities. These electron densities are rather different from the Mulliken populations shown later (Fig. 8); Mulliken populations attribute the total population of each basis function (BF) to the centre carrying the BF, irrespective of the spatial distribution of the electron density; however, it is important to note that the *same wave-functions* are used as in the AIM procedure.

The most obvious features of the AIM densities, for both types of compound, azines **11–14** and the *N*-oxides **7–10** (Fig. 6), is that the H-atoms are relatively close to neutral. The C–H bonds have very low Cδ(–)–Hδ(+), dipoles,⁵² where δ < 0.1e with the dipole bond direction shown. However, an *N*-atom attached to C causes a large bond dipole Cδ(+)-Nδ(–), in the azines **11–14** where δ is 0.53e–0.56e. This is repeated in the *N*-oxides, where a high charge density occurs at both N₁ and N₄ in pyrazine *N*-oxide **10**, for example. This is clearly not a result of the *N*-oxide group, since in pyridine *N*-oxide, no similar effect occurs. Indeed, the C₂ atoms in the *N*-oxides **7–10** have much lower positive charge (~0.4e) than other C-atoms; this suggests that the *N*-oxide is actually a donor to C₂/C₆ rather than C₄ in the ground state molecule. If we compare the *N*-oxide directly with the corresponding azine, e.g., **7** with **11** etc. (Fig. 7), we find that the O-atom of the *N*-oxides **7, 9** and **10** carry a negative charge of –0.50e to 0.55e, with the attached *N*-atom +0.60e. In the case of the pyridazines (**8**), the Oδ(–)–Nδ(+)
dipole is smaller, and part of the electron density is transferred to the adjacent N₂ atom. Using the same oxide/azine comparisons, the *ortho* C-atoms show a surplus density of ~0.15e in each pair of compounds (**7,11**; **8,12**; **9,13**; **10,14**). However, this completes the main charge re-distribution in the *N*-oxides; the *meta* C-atoms carry a small electron deficiency, with the same at the *para* sites.

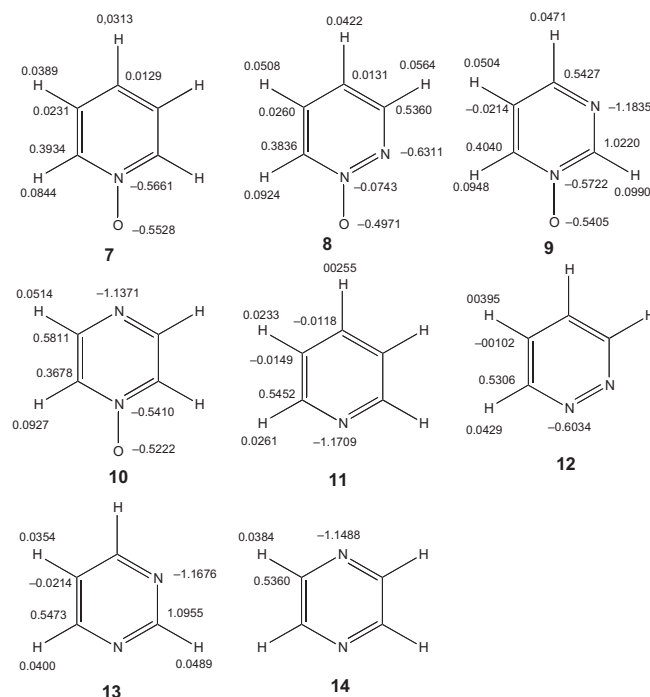


Fig. 6. AIM charges at the atomic centres based on electron density summations.

There is clearly *no indication* that an *N*-oxide group enhances the electron density at the *para* centre in the ground state molecules. The enhanced *para* reactivity must therefore be a polarisation effect at the time of reaction with an electrophile.

The Mulliken charge densities are shown in Fig. 8. As discussed above, the distributions, being based on quite different criteria, do show a number of similarities to the AIM total electron densities, and both have a use in rationalisation of spectral and reactivity data however, and hence the Mulliken populations are discussed in this Section. The electron density in pyridine- and pyrimidine *N*-oxides are fairly similar, as expected on molecular orbital grounds, where the back-donation from oxygen is through the π-system, and the *meta*-orientation of the *N*-atoms leads to a weak interaction.

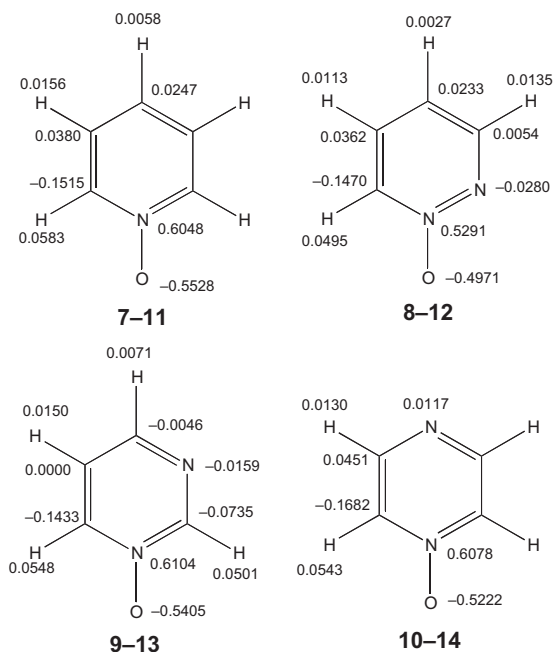


Fig. 7. Electron density differences between azine *N*-oxide and corresponding azine.

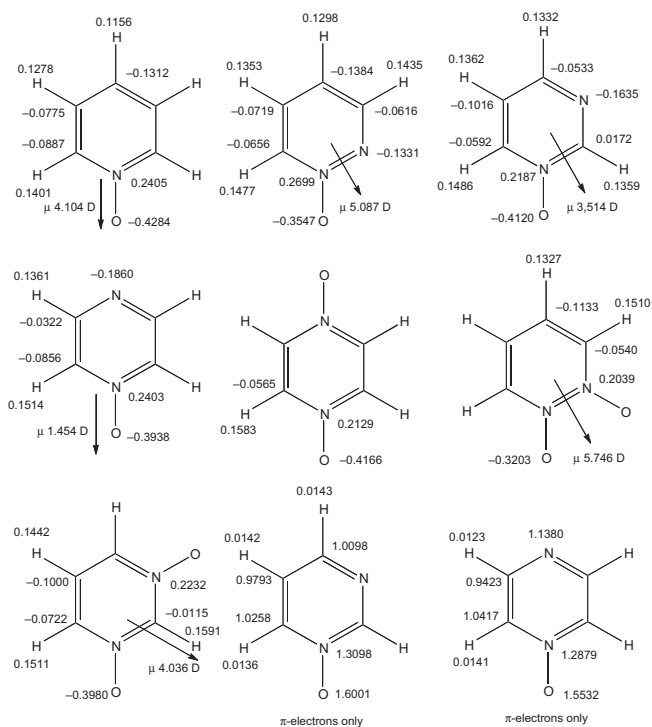


Fig. 8. Calculated Mulliken charges and dipole moments.

The ease of electrophilic substitution at C₄ in pyridine *N*-oxide has long been attributed to back-donation as in **6**. The present data in Fig. 8 shows that although the 8π-electron system undergoes considerable reorganisation from the classical N⁽⁺⁾–O^(–) representation, only about 0.4e is lost from the O-atom, and most of that is localised on the N-atom, thereby reducing the positive charge. This situation is very similar to the AIM results. For pyrazine *N*-oxide, the additional N-atom draws a further charge to the N₄ position, but otherwise the effects are small. Thus if we take the difference in Mulliken atomic populations at each centre between pyrazine *N*-oxide and pyrazine, we obtain the following (approximate) values: O₁ –0.39, N₁ +0.39, N₄ –0.03, C₂/C₆ –0.03, C₃/C₅ +0.02, H₂/H₆ +0.02, H₃/H₅ 0.00e. After allowance for the electron distribution in the azines (Fig. 7), these figures are somewhat similar to the AIM conclusions. The extent of this back-bonding seems general for these compounds, and is largely localised in the O→N moiety.

However, a further effect, which will have a significant effect on the reactivity in the *N*-oxides is the Madelung potential (Eq.1), where the presence of internal electric dipoles in the molecule have a distinct effect on both the electron density and the potential at the nucleus.⁴² The potential energy and electron density are modified by a local dipole (q_i) at an angle ϑ_i and at a distance r_i from the centre (i), as in Eq. 1 Clearly this term is maximal when the cosine is unity, i.e., in line with the centre under scrutiny. This situation applies to the *para* position of the azine *N*-oxides in particular, because of the very high bond dipoles, but is less elsewhere in the molecules. It provides a partial interpretation of the higher electron density at N₄ than is given by the Mulliken populations.

$$\Delta E = \sum_i \frac{q_i \cos \vartheta_i}{r_i} \quad (1)$$

5. Conclusions

The credibility of the theoretical structures is demonstrated by comparison with microwave structures for the azines; the

close relationship between the dipole moments, as determined theoretically and by experiment, extends this conclusion to the electron distributions. The variation in bond lengths and angles with structure show systematic effects in the theoretical study, and some of these are reflected in the experimental crystal structures. The limitations of these comparisons probably arise from the effects of neighbour *N*-oxide molecules in the solid state, and in particular to the dipole–dipole interactions, which occur.

The charge densities in the *N*-oxides have been a matter for discussion, and we have endeavoured to both rationalise the substituent effects across the series of compounds, and draw attention to difference between the total electron density (AIM) and the Mulliken populations.

The ready reactivity of the pyridine *N*-oxide at C₄ to electrophiles, is most likely to be due to a polarisation effect in the presence of the reagent, rather than to a high electron density at that centre.

All of the above study relates to ground state properties, and in particular to structural features, such as bond lengths and angles, and their relationship to theoretical results by the two main methods available to computational chemists, namely AIM and Mulliken analyses.

The differences between these methods are significant, and this must be understood to avoid the conclusion that there is only one measure of electron density in a molecule. The density integration procedure in AIM is clearly not practicable for large molecules, since it would require summations at many centres. In those circumstances, the Mulliken method of summing the density in individual molecular orbitals, about the centre where the basis function is centred, is clearly much more easily scalable to large molecules. Provided that there are only valence type functions, the AIM and Mulliken methods may well give similar results; however, when diffuse functions are employed, as is necessary for charged species and very polar molecules, the two methods can give very different results, and we see that occurring here.

Now the question of reactivity raises further issues, and in the case of the *N*-oxides, it is facile electrophilic substitution at positions *para* to the *N*-oxide, which is the group characteristic. Both in acid catalysed proton exchange and nitration we are probably comparing the pyridinium cation (C₅H₅NH⁺) with the *N*-hydroxypyridinium cation (C₅H₅NOH⁺). The former must have a deficiency in electron density available at the 2- and 4-positions for electron donation to an incoming electrophile. The latter in contrast is closer to the situation in a phenol, where ready electrophilic substitution occurs.

There is no doubt that *para*-localisation energy is facilitated at C₄ in pyridine *N*-oxide **1**; in the case of proton exchange at that position, a tetrahedral C₄ centre is generated by out of plane attack by the incoming electrophilic H⁺ in this instance (or NO₂⁺ in nitration). π-Electron release from the *N*-oxide oxygen atom must be significantly easier than from the protonated ring NH⁺ of the pyridine ring, owing to the high π-electron density on the N–O or even N–OH⁺ groups.

6. Experimental section

6.1. General

NMR spectra were run at 300 MHz using a Bruker Avance 500 instrument on solutions in CDCl₃ with internal Me₄Si as reference. Chemical shifts are reported in parts per million to high frequency of the reference and coupling constants J are in Hertz. Melting points were determined on a Reichert hot-stage microscope.

6.2. Synthesis

6.2.1. Pyridazine N-oxide 2.³ A solution of pyridazine (2.0 g, 25 mmol) and mCPBA (8.625 g, 50%, 25 mmol) in CH₂Cl₂ (150 mL) was stirred at rt for 48 h. Addition of Ph₃P (3.275 g, 12.5 mmol), stirring for a further 4 h, then evaporation and chromatography of the residue (SiO₂, EtOAc to 20% MeOH in EtOAc) gave a major fraction consisting of a mixture of product and starting material. Vacuum distillation of this gave unreacted pyridazine followed by the title product (1.62 g, 68%) as a colourless liquid, bp 175 °C at 20 Torr; δ_H 7.19 (1H, ddd, J 7.5, 5.1, 1.0), 7.76 (1H, m), 8.24 (1H, dt, J 6.3, 1.0) and 8.52 (1H, m). The product solidified upon cooling (lit.⁶ mp 38–39 °C) and crystals suitable for X-ray diffraction were obtained from Et₂O by cooling at –78 °C.

6.2.2. Pyrimidine N-oxide 3. Pyrimidine was prepared by a literature method.⁵³ A solution of pyrimidine (1.25 g, 15.6 mmol) and mCPBA (5.38 g, 50%, 15.6 mmol) in EtOAc (150 mL) was heated under reflux for 4 h. Evaporation followed by chromatography of the residue (SiO₂, 15% MeOH in EtOAc) gave the title product (0.51 g, 34%) as colourless crystals, mp 82–84 °C (lit.⁶ 95–96 °C); δ_H 7.28 (1H, ddd, J 6.6, 4.8, 1.0), 8.22 (1H, dd, J 4.8, 1.5), 8.37 (1H, ddd, J 6.6, 2.1, 1.5) and 8.96 (1H, dd, J 2.1, 1.0).

6.2.3. Pyrazine N-oxide 4.⁶ A solution of pyrazine (2.5 g, 31 mmol) in AcOH (30 mL) was stirred at 70–80 °C while a mixture of 30% H₂O₂ (3.55 g, 32 mmol) and AcOH (25 mL) was added dropwise over 30 min. After the addition, heating was continued for 5 h then the mixture was evaporated under reduced pressure and the residue was taken up in CH₂Cl₂ (125 mL). Drying over anhydrous Na₂CO₃ and evaporation gave a solid, which was recrystallised from hexane to give the title product (1.48 g, 50%) as colourless crystals, mp 113–114 °C (lit.⁶ 113–114 °C); δ_H 8.11 (2H, m) and 8.48 (2H, m).

6.3. Crystallography

X-ray diffraction data were recorded on a Rigaku diffractometer with MoKα radiation (λ=0.71073 Å). The structures were solved by direct methods and refined using full-matrix least-squares methods.

Crystal data for 2: C₄H₄N₂O, M=96.09, colourless platelet, crystal dimensions 0.30×0.05×0.05 mm, monoclinic, space group P2₁/n, a=3.819(4), b=9.993(5), c=22.171(8) Å, β=90.72(2)°, V=846.0(10) Å³, Z=8, D_c=1.509 Mg m⁻³, T=93(2) K, R=0.2412, R_w=0.5926 for 1142 reflections with I>2σ(I) and 129 variables.

Crystal data for 3: C₄H₄N₂O, M=96.09, colourless prism, crystal dimensions 0.10×0.05×0.05 mm, monoclinic, space group P2₁/n, a=5.437(3), b=4.0051(19), c=19.440(10) Å, β=95.443(17)°, V=421.4(4) Å³, Z=4, D_c=1.515 Mg m⁻³, T=93(2) K, R=0.0619, R_w=0.1567 for 603 reflections with I>2σ(I) and 66 variables.

Crystal data for 4: C₄H₄N₂O, M=96.09, colourless prism, crystal dimensions 0.20×0.10×0.06 mm, monoclinic, space group P2₁/n, a=11.416(3), b=3.6545(10), c=20.889(6) Å, β=91.970(7)°, V=871.0(4) Å³, Z=8, D_c=1.466 Mg m⁻³, T=93(2) K, R=0.0628, R_w=0.1619 for 1216 reflections with I>2σ(I) and 129 variables.

Crystallographic data (excluding structure factors) for the structures in this paper have been deposited with the Cambridge Crystallographic Data Centre as supplementary publication nos. CCDC 865893 (2), 865894 (3) and 865895 (4).⁵⁴

References and notes

- Ochiai, E. *J. Org. Chem.* **1953**, *18*, 534–551.
- Eichhorn, E. L. *Acta Crystallogr.* **1956**, *9*, 787–793.

- Leclerc, J.; Fagnou, K. *Angew. Chem., Int. Ed.* **2006**, *45*, 7781–7786.
- Moore, P. R.; Mannering, G. J.; Teply, L. J.; Kline, B. E. *Cancer Res.* **1960**, *20*, 628–634.
- Munoshiba, T.; Demple, B. *Cancer Res.* **1993**, *53*, 3250–3252.
- Koelsch, C. F.; Gumprecht, W. H. *J. Org. Chem.* **1958**, *23*, 1603–1606.
- Ülkü, D.; Huddle, B. P.; Morrow, J. C.; Marsh, R. E. *Acta Crystallogr., Sect. B* **1971**, *27*, 432–436.
- Kapon, M.; Hu, S.; Herbstein, F. H. *Acta Crystallogr., Sect. B* **2002**, *58*, 62–77.
- Näther, C.; Kowallik, P.; Jess, I. *Acta Crystallogr., Sect. E* **2002**, *58*, o1253–o1254.
- Snerling, O.; Nielsen, C. J.; Nygaard, L.; Pedersen, E. J.; Sorensen, G. O. *J. Mol. Struct.* **1975**, *27*, 205–211.
- Sorensen, G. O.; Tang-Pedersen, A.; Pedersen, E. J. *J. Mol. Struct.* **1983**, *101*, 263–268.
- Heineking, N.; Dreizler, H.; Endo, K.; Kamura, Y. *Z. Naturforsch., A* **1989**, *44*, 1196–1200.
- Chiang, J. F. *J. Chem. Phys.* **1974**, *61*, 1280–1283.
- Sato, N.; Matsumoto, K.; Takishima, M.; Mochizuki, K. *J. Chem. Soc., Perkin Trans. 1* **1997**, 3167–3172.
- Kucharski, T. J.; Oxsher, J. R.; Blackstock, S. C. *Tetrahedron Lett.* **2006**, *47*, 4569–4572; Cong, Q.; Lin, S.; Wang, H. *Jiegou Huaxue* **1989**, *8*, 31–35.
- Fruttero, R.; Ferrarotti, B.; Gasco, A.; Calestani, G.; Rizzoli, C. *Liebigs Ann. Chem.* **1988**, 1017–1023.
- Palmer, M. H.; Russell, E. R. *R. Chem. Ind. (London)* **1965**, 157–158.
- Suzuki, I.; Nakadate, M.; Sueyoshi, S. *Tetrahedron Lett.* **1968**, *9*, 1855–1868.
- Katritzky, A. R.; Randall, W.; Sutton, L. E. *J. Chem. Soc.* **1957**, 1769–1775.
- Soscún, H.; Castellano, O.; Bermúdez, Y.; Toro-Mendoza, C.; Marcanob, A.; Alvarado, Y. *J. Mol. Struct.: THEOCHEM* **2002**, *592*, 19–28.
- Sorensen, G. O.; Mahler, L.; Rastrup-Andersen, N. *J. Mol. Struct.* **1974**, *20*, 119–126.
- Pyckhout, W.; Horemans, N.; Van Alsenoy, C.; Geise, H. J.; Rankin, D. W. H. *J. Mol. Struct.* **1987**, *156*, 315–329.
- Mootz, D.; Wussow, H.-G. *J. Chem. Phys.* **1981**, *75*, 1517–1522.
- Mata, F.; Quintana, M. J.; Soerensen, G. O. *J. Mol. Struct.* **1977**, *42*, 1–5.
- Blake, A. J.; Rankin, D. W. H. *Acta Crystallogr., Sect. C* **1991**, *47*, 1933–1936.
- Werner, W.; Dreizler, H.; Rudolph, H. D. *Z. Naturforsch., A* **1967**, *22*, 531–543.
- Innes, K. K.; Lucas, R. M. *J. Mol. Spectrosc.* **1967**, *24*, 247–250.
- Almenningen, A.; Bjoernsen, G.; Ottersen, T.; Seip, R.; Strand, T. G. *Acta Chem. Scand.* **1977**, *A31*, 63–68.
- Cradock, S.; Purves, C.; Rankin, D. W. H. *J. Mol. Struct.* **1990**, *220*, 193–204.
- Cradock, S.; Liescheski, P. B.; Rankin, D. W. H.; Robertson, H. E. *J. Am. Chem. Soc.* **1988**, *110*, 2758–2763.
- Furberg, S.; Groegaard, J.; Smedsrud, B. *Acta Chem. Scand. B* **1979**, *33*, 715–724.
- Blackman, G. L.; Brown, R. D.; Burden, F. R. *J. Mol. Spectrosc.* **1970**, *35*, 444–454.
- Khetrapal, C. L.; Patankar, A. V.; Diehl, P. *Org. Magn. Reson.* **1970**, *2*, 405–407.
- Wheatley, P. J. *Acta Crystallogr.* **1957**, *10*, 182–187.
- de With, D.; Harkema, S.; Feil, D. *Acta Crystallogr., Sect. B* **1976**, *32*, 3178–3184.
- Bormans, B. J. M.; De With, G.; Mijlhoff, F. C. *J. Mol. Struct.* **1977**, *42*, 121–128.
- Palmer, M. H.; Nelson, A. D. *J. Mol. Struct.* **2006**, *825*, 93–100.
- Palmer, M. H.; Nelson, A. D. *J. Mol. Struct.* **2006**, *782*, 94–105.
- Frisch, M. J.; Trucks, G. W.; Schlegel, H. B.; Scuseria, G. E.; Robb, M. A.; Cheeseman, J. R.; Montgomery, J. A., Jr.; Vreven, T.; Kudin, K. N.; Burant, J. C.; Millam, J. M.; Iyengar, S. S.; Tomasi, J.; Barone, V.; Mennucci, B.; Cossi, M.; Scalmani, G.; Rega, N.; Petersson, G. A.; Nakatsuji, H.; Hada, M.; Ehara, M.; Toyota, K.; Fukuda, R.; Hasegawa, J.; Ishida, M.; Nakajima, T.; Honda, Y.; Kitao, O.; Nakai, H.; Klene, M.; Li, X.; Knox, J. E.; Hratchian, H. P.; Cross, J. B.; Bakken, V.; Adamo, C.; Jaramillo, J.; Gomperts, R.; Stratmann, R. E.; Yazyev, O.; Austin, A. J.; Cammi, R.; Pomelli, C.; Ochterski, J. W.; Ayala, P. Y.; Morokuma, K.; Voth, G. A.; Salvador, P.; Dannenberg, J. J.; Zakrzewski, V. G.; Dapprich, S.; Daniels, A. D.; Strain, M. C.; Farkas, O.; Malick, D. K.; Rabuck, A. D.; Raghavachari, K.; Foresman, J. B.; Ortiz, J. V.; Cui, Q.; Baboul, A. G.; Clifford, S.; Cioslowski, J.; Stefanov, B. B.; Liu, G.; Liashenko, A.; Piskorz, P.; Komaromi, I.; Martin, R. L.; Fox, D. J.; Keith, T.; Al-Laham, M. A.; Peng, C. Y.; Nanayakkara, A.; Challacombe, M.; Gill, P. M. W.; Johnson, B.; Chen, W.; Wong, M. W.; Gonzalez, C.; Pople, J. A. *Gaussian 03, AM64L-G03RevD.01*; Gaussian: Wallingford CT, 2004.
- Dunning, T. H., Jr. *J. Chem. Phys.* **1989**, *90*, 1007–1023.
- Bader, R. F. W. *Atoms in Molecules – a Quantum Theory*; Clarendon: Oxford, 1990; p 259.
- van der Avoird, A. *Chem. Commun.* **1970**, 727–728.
- Mulliken, R. S. *J. Chem. Phys.* **1955**, *23*, 1833–1840.
- Brown, R. D.; Burden, F. R.; Garland, W. *Chem. Phys. Lett.* **1970**, *7*, 461–462.
- Mosher, H. S.; Turner, L.; Carlsmith, A. *Org. Synth.* **1953**, *33*, 79–81.
- Heiberg, A. B.; Talberg, H. *J. Adv. Mol. Relax. Processes* **1977**, *9*, 199–210.
- Germain, G.; Piret, P.; Van Meerse, M. *Acta Crystallogr.* **1963**, *16*, 109–112.
- Olsson, L.; Cremer, D. *J. Phys. Chem.* **1996**, *100*, 16881–16891.
- Kubota, T.; Watanabe, H. *Bull. Chem. Soc. Jpn.* **1963**, *36*, 1093–1096.
- Ogata, M.; Watanabe, H.; Tori, K.; Kano, H. *Tetrahedron Lett.* **1964**, *5*, 19–24.
- Biegler König, F. W.; Bader, R. F. W.; Tang, T. *J. Comput. Chem.* **1982**, *13*, 317–328.
- Palmer, M. H.; Findlay, R. H.; Gaskell, A. J. *J. Chem. Soc., Perkin Trans. 2* **1974**, 420–428.
- Bredereck, H.; Gompper, R.; Morlock, G. *Chem. Ber.* **1957**, *90*, 942–952.
- Copies of the data can be obtained, free of charge, on application to CCDC, 12 Union Road, Cambridge CB2 1EZ, UK, (fax: +44 (0) 1223 336033 or e-mail: deposit@ccdc.cam.ac.uk).